Hindawi
Geofluids
Volume 2023, Article ID 6485987, 14 pages
https://doi.org/10.1155/2023/6485987

Research Article

Mechanism and Control of Water–Rock Coupling-Induced Disaster when Mining below the Unconsolidated Confined Aquifer

Zhihua Li,[1,2,3] **Ke Yang**,[1,2,3] **Xinzhu Hua**,[1,2,3] **Cheng Liu**,[1,2,3] **Peng Zhou**,[1,2,3] **and Shengwen Ge**[4]

[1]*School of Mining Engineering, Anhui University of Science and Technology, Huainan 232001, China*
[2]*Key Laboratory of Coal Mine Safety and Efficient Mining of Ministry of Education, Anhui University of Science and Technology, Huainan 232001, China*
[3]*Institute of Energy, Hefei Comprehensive National Science Center, Hefei 230031, China*
[4]*Panji No. 2 Coal Mine, Huainan Mining Group, Huainan 232096, China*

Correspondence should be addressed to Zhihua Li; lizhihua81@126.com

Received 10 September 2022; Revised 7 October 2022; Accepted 11 October 2022; Published 24 January 2023

Academic Editor: Zhengzheng Xie

Theoretical analysis and numerical simulation were conducted to study the disaster-causing mechanism of structural instability of the overlying strata induced by water–rock coupling and effectively prevent and control the powered support jammed accident during mining below the unconsolidated confined aquifer. The influencing factors on the stability of the overlying strata structure were analyzed, and the numerical simulation method of unconsolidated confined aquifer was designed. The disaster-causing mechanism and the evolution process of the stress–displacement–crack field of the overlying strata induced by water–rock coupling were discovered. Meanwhile, the prevention measures for the structural instability of the overlying strata were proposed and verified in some engineering practice. Results show that the stability of the overlying strata structure reduces with the increase in hydraulic pressure, the breaking interval of the main roof, and the decrease in the overlying strata strength and waterproof coal pillar height. The overlying strata structure keeps a stable equilibrium state before the fracture planes through a whole waterproof coal–rock pillar. When the hydraulic pressure is small or the bedrock surface is a thick topsoil layer, the sliding block is in a state of limit equilibrium for the decrease of pressure on the sliding block while the fracture planes through a whole waterproof coal–rock pillar because of the action of unloading during an overlying strata movement. When the hydraulic pressure is high, the pressure on the sliding block remains constant at about hydraulic pressure, and the intact shear fall of the sliding block occurs as a result of the hydraulic pressure of the confined aquifer and the weight of the sliding block, which may result in a powered support jammed accident. However, this type of accident can be prevented by drainage for decreasing hydraulic pressure, presplitting blasting of the hard main roof, overlying strata grouting reinforcement, and increasing the height of the waterproof coal–rock pillar.

1. Introduction

The mining seams in Eastern China, North China, and Northeast China are covered with an approximately 200–600 m thick unconsolidated confined aquifer. According to studies, 80 m waterproof coal–rock pillars are frequently reserved in the early stage, and the coal loss exceeds 10 billion tons [1]. The coal series and bedrock strata in Anhui Huainan Panji Xieqiao Mining area are covered by 120–484 m thick Cenozoic loss beds. The lower gravel aquifer directly contacts with the coal series, resulting in mining under high water head conditions [2]. Accordingly, the 80 m waterproof coal–rock pillars were preset in all mines during the design, and the reverses of the waterproof coal–rock pillars reach 600 million tons [3]. Shrinking the waterproof coal–rock pillars and increasing the upper limit

mining can prolong the length of the level-1 services of mines, relieve the tense replacement, and increase recovery of coal resources [4]. With the continuous progresses of mining technologies below "railways, buildings, and water bodies," many mines have decreased the height of waterproof coal–rock pillars from the original 80 m to 20–30 m. Most working faces have achieved successful recovery. However, some working faces have suffered powered support jammed accidents. For example, working faces 1402(3) and 1602(3) in Panyi Mine, Huainan, working face $1711_0(3)$ in Pansan Mine, and working face 1202(3) in Gubei Mine had serious powered support jammed accidents at the first weighting, thus causing considerable economic losses [5, 6].

Recently, Chinese scholars have carried out a number of experimental studies and theoretical analyses on the feasibility of safe mining under unconsolidated confined aquifer, strata pressure behavioral laws of the working faces, overlying strata structure of stope, disaster-causing mechanism of powered support jammed, and determination of the reasonable working resistance of the powered support and risk control technology of the powered support jammed. These studies promoted basic theoretical studies on underground pressure and development of strata control technology. Yuan and Liu [2] analyzed and predicted the mining of shrunk waterproof pillar in Huainan Panji Mine. Zhang et al. [3] believed that layered mining was applied in Panji Mine, the waterproof coal–rock pillars can be reduced to 40 m. Li [4] suggested to replace existing waterproof coal–rock pillars by fully using the bottom clay water-resisting layer of the aquifer as waterproof rock pillars. Li et al. [7] proposed an evaluation method of powered support jammed risks in working faces based on the comprehensive index method. Yang et al. [8] pointed out the characteristics of strata pressure behaviors in the working faces below confined aquifer, such as strong static pressure, small dynamic pressure. Xu et al. [9, 10] believed that the key strata can easily develop composite breakage due to the load transmission effect of the unconsolidated confined aquifer, thus causing sliding instability of the "Voussoir beam" structure. Hou et al. [11] divided the stope into three types according to the bedrock and mining height ratio, including "plate-shell type," "plate and no shell type," and "no plate, no shell." Zhang et al. [12] believed that large-scaled collapse and sinking of the overlying strata occurred on the single key strata due to the load transmission of the loose aquifer, which easily causes support jammed accidents. Meng et al. [13] discussed the four stages of crack propagation under different lengths of the original cracks, overlying strata pressure, and water and sand effects and provided the failure curves. Zhang et al. [14] analyzed and tested the initial crack distribution features in the blocking strata and crack distribution features in the deformation failure process. Zhang et al. [15] pointed out that buckling of the waterproof soil layer is closely related with mining parameters under the condition of thin bedrock. Xu et al. [16] believed that the mining-induced cracks of the mudstone in the weathering zone were expanded into pipelines due to the high hydraulic pressure. Wang et al. [17] believed that the repetitive mining overlying strata under the unconsolidated confined aquifer make the overall failure unlikely to develop, thus decreasing the risk of the water inrush and power support jammed. Wang et al. [18] proposed support crushing and water inrush when mining under an unconsolidated confined aquifer can been prevented by roof preblasting.

Chinese scholars have carried out many studies on mining under the unconsolidated confined aquifer and achieved a group of important research results. However, previous studies paid little attention to the moving features of the overlying strata, stress transfer law, and development and propagation of the fracture surface. An instability mechanical model of the overlying strata structure with the water–rock coupling effect was constructed in this study according to the moving features of the overlying strata under the unconsolidated confined aquifer. The stress–displacement–crack evolutionary process of the stope and the disaster-causing mechanism under the water–rock coupling effect was disclosed. Meanwhile, the instability control technology of the overlying strata structure was proposed.

2. Water–Rock Coupling-Induced Disaster Mechanism

2.1. Stability Analysis of Water–Rock Coupling Overlying Strata Structure. The roof cut fell along the coal wall when power support jammed accidents occurred in the shallow coal seam, resulting in the collapse of the stairs on the surface [19, 20]. This phenomenon indicates that mining-induced cracks formed by rock strata movement ran through the whole overlying strata, and breakage of the key strata leads to the overall movement of the overlying strata [21]. When power support jammed accidents of working faces occurred under the unconsolidated confined aquifer in the eastern regions, the roof stairs sunk along coal wall of the working faces, which is often accompanied with water inrush accidents. Specifically, the fracture surface formed by movement of rock strata has run through the confined aquifer, and breakage of the key strata may result in the overall movement of the waterproof coal–rock pillars. An instability mechanical model with the water–rock coupling effect was constructed according to the moving characteristics of the overlying strata under an unconsolidated confined aquifer (Figure 1).

Whether the breaking block B of the key stratum can form a stable "Voussoir beam" structure is mainly related with loads on the key strata [21]. If the loads on the key strata are stronger, then the "Voussoir beam" structure formed by the broken rocks can easily develop sliding instability [22]. Complete and continuous overlying strata are impossible to form because the shallow rock of the thin bedrock is influenced by weathering. The overlying strata are believed to have loose bodies and some cohesion. The stratum strength adheres to the Mohr–Coulomb strength criterion [22]. At the first weighting of the working face, the fracture surface on the overlying strata in the stope can be approximately viewed as a vertical plane that extends to the confined aquifer [22]. Under such overlying structural forms, the loads applied by the sliding bodies CDEF onto

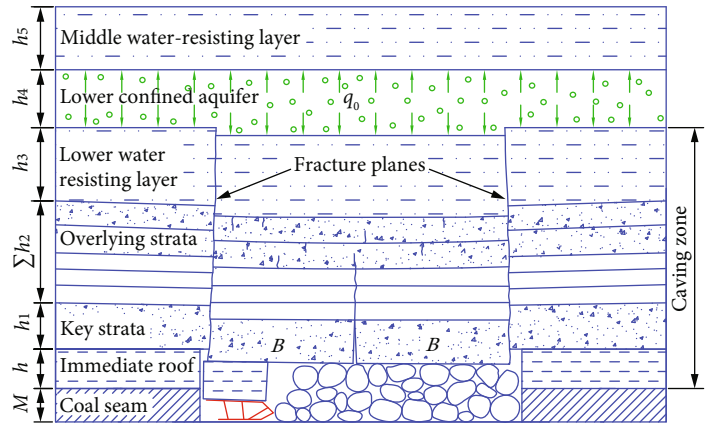

Figure 1: Mechanical model of the water–rock coupling induced disaster.

the key strata can be calculated by using the Terzaghi theory (Figure 2).

The surrounding rock pressure on the broken rocks in the key strata (q_s) was [23]

$$q_s = \frac{a\gamma - c_j}{\lambda \tan \phi_j}\left[1 - e^{-\lambda \tan \phi_j / a \times H}\right] + q_0 e^{-\lambda \tan \phi_j / a \times H}, \quad (1)$$

where q_0 is the hydraulic pressure (MPa), H the distance from the key strata to the confined aquifer (m), $2a$ the breaking interval on the key strata (m), λ the coefficient of horizontal pressure, c_j the cohesion of the fracture plane (MPa), φ_j the internal friction angle of the fracture plane (°), and γ refers to the average volume weight of overlying strata (MN/m^3).

2.2. Influencing Factor Analysis of Water–Rock Coupling Induced Disasters. Equation (1) shows that the major influencing factors of the overlying loads of the key strata include hydraulic pressure of the confined aquifer, first weighting interval of working faces, and height of the waterproof pillars, strength parameters of the fracture surface. The influences of the abovementioned parameters on the overlying loads of the key strata were discussed by using the single-factor sensitivity analysis method to analyze water–rock coupling induced disaster mechanism ($q_0 = 3.0$ MPa, $H = 60$ m, $2a = 20$ m, $\lambda = 1$, $c_j = 0.2$ MPa, $\varphi_j = 20\circ$, and $\gamma = 0.024$ MN/m^3).

2.2.1. Hydraulic Pressure of the Unconsolidated Confined Aquifer. The coal measure strata in Huainan Mine are covered by 120–484 m thick Cenozoic loose layers, and the gravel aquifer below it directly contacts with the coal series, thus resulting in mining under high water head condition (2). The variation and fitting curves of the overlying load on the key strata with hydraulic pressures are represented in Figure 3. The overlying load on the key strata has a linear relation with the hydraulic pressure of the confined aquifer. This load increases with the increase in hydraulic pressure. Moreover, the regression equation shows that only 0.112 times of hydraulic pressure may be transferred to the key

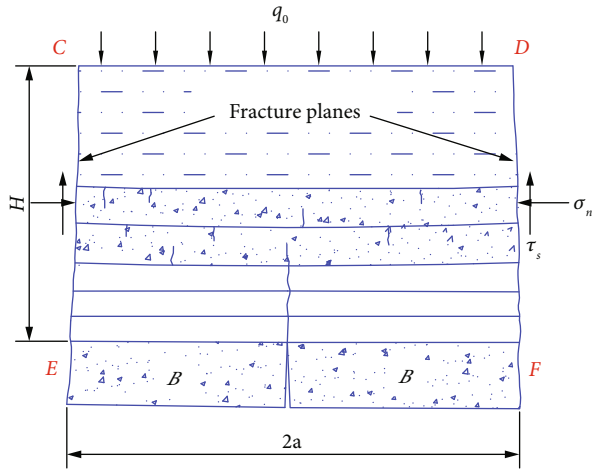

Figure 2: Calculation of the surrounding rock pressure based on the Terzaghi theory [22].

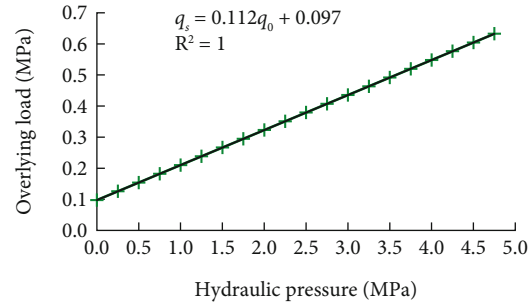

Figure 3: Change curves of pressure on the key strata with different hydraulic pressures.

strata through the overlying strata when the waterproof coal pillar is 60 m. The overlying load is about 0.1 MPa when the hydraulic pressure is 0, which is the load component of pillar's dead loads on the key strata.

2.2.2. Breaking Interval of the Main Roof. The breaking of the key strata causes the entire or a portion of the overlying

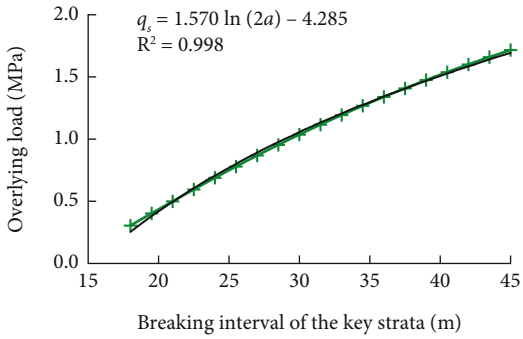

Figure 4: Change curves of pressure on the key strata with different first breaking intervals.

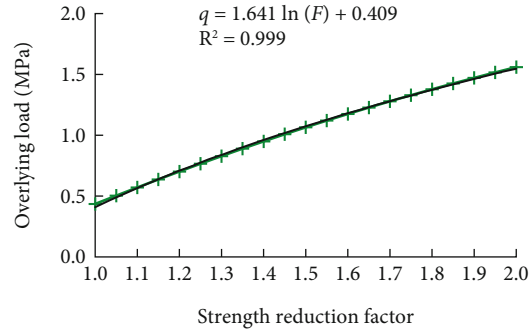

Figure 5: Change curves of pressure on the key strata with different strength reduction factors.

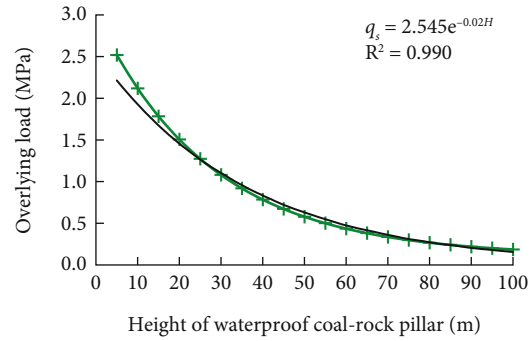

Figure 6: Change curves of pressure on the key strata with different heights of waterproof coal–rock pillars.

strata to move [21]. Moreover, the movement of the overlying strata may influence the overlying loads of the key strata. The variation and fitting curves of the overlying loads of the key strata under different breaking intervals are shown in Figure 4. The overlying load on the key strata has a logarithmic relationship with the breaking interval of key strata. This load increases with the increase in the breaking interval of the key strata. However, the growth rate gradually decreases. A larger breaking interval can be observed on the working faces with thin bedrock if the main roof is thicker and stronger. Accordingly, the overlying load on the key strata increases after breakage of the main roof.

2.2.3. Strength of the Overlying Strata. The strength reduction method is applied. First, the strength reduction factor (F) is chosen to reduce the strength parameters (cohesion c_j and internal friction angle φ_j) of the overlying strata joint surface according to Equation (2). Next, the reduced strength parameters are brought into Equation (1) for calculation. The variation and fitting curves of the overlying loads under different reduction coefficients can be obtained (Figure 5).

$$c_j' = \frac{c_j}{F} \quad \phi_j' = \arctan\left(\frac{\tan\phi_j}{F}\right). \tag{2}$$

Figure 5 shows that the overlying load of the key strata has a logarithmic relationship with the strength reduction factor of the fracture plane. The load increases with the increase in the strength reduction factor due to weathering and oxidization. Accordingly, the broken rocks on the key strata can easily develop sliding instability.

2.2.4. Height of the Waterproof Coal–Rock Pillars. The variation and fitting curves of the overlying loads of the key strata under different heights of waterproof coal pillars are shown in Figure 6. The aforementioned figure demonstrates that the overlying load on the key strata has a negative exponential relationship with the waterproof coal pillars. When the key strata is close to the aquifer layer, the overlying loads of the key strata dramatically decrease with the increase of the waterproof coal pillars. However, the reduction amplitude of the overlying load decreases with the increase of the waterproof coal pillars when the distance between the key strata and the aquifer layer is larger than 80 m [22]. This phenomenon indicates that when the waterproof coal pillars is large, the overlying load of the key strata slightly changes by decreasing the height, but it may dramatically increase after the height is decreased to a certain value.

3. Numerical Simulation of Water–Rock Coupling Overlying Structural Instability

3.1. Engineering Background. On working face 1202(3) in Huainan Gubei Mine, the minimum waterproof coal–rock pillars locate on the upper end of the cutting eye, where the elevations of the bedrock surface and roof are −462.9 and −490.5 m, respectively. Moreover, the height of the minimum waterproof coal pillars is 27.6 m, and the minimum water-resisting layer is 27.4 m. The minimum waterproof coal–rock pillars is 55 m high [5].

The mining of 1202(3) working face started on May 12, 2011, and it was advanced for 30 m (including the 6 m of cutting eye) on May 16, 2011 (Figure 7). The middle and upper parts of the working face were under sudden pressure. The safety valves on the supports were all turned on. Most rear pillars of the support had no strokes. This accident caused 52 supports on the working face to collapse, necessitating the dismantling of the working face in advance [5].

3.2. Numerical Model

3.2.1. Construction of a Numerical Model. A numerical simulation model was constructed using the UDEC discrete

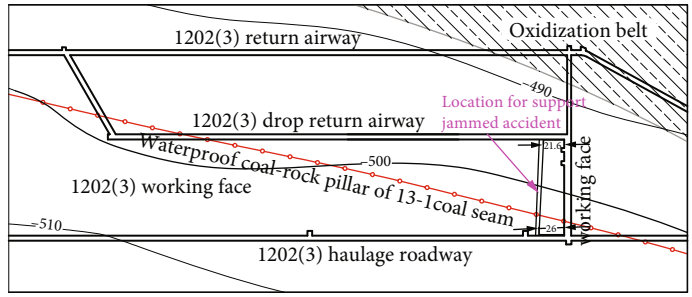

Figure 7: Layout plan of 1202(3) working face.

element software based on the engineering geological of 1202(3) working face (Figure 8). The coal seam dip angle was 3°–7°, as an approximately flat coal seam. The model was 180 m in width and 150 m in height. The left and right sides restrict horizontal displacements. The lower boundary restricts the vertical displacement. The upper boundary applies a 9.75 MPa load to simulate the external loads of the loose layer. The physical mechanical properties of the coal and rock are listed in Table 1. The mechanical properties of the joint surface are listed in Table 2. The Mohr–Coulomb model and the Coulomb-slip model were applied [24, 25].

3.2.2. Numerical Simulation of the Hydraulic Pressure. Secondary development was carried out based on the FISH embedded language in the 2D discrete element calculation software UDEC program. During the balanced operation of the model, the program has to judge whether the surrounding rock pressure (q) on the top boundary of the lower water-resisting layer is smaller than the hydraulic pressure (q_0) of the confined aquifer. According to the judgment results, the two optional treatments are as follows: if $q < q_0$, then a compensation force ($\Delta q = q_0 - q$) is applied onto the top boundary of the lower water-resisting layer through the internal stress boundary command, and the model continues to make a balance operation. If $q > q_0$, then the model can directly make the balance operation.

3.3. Numerical Simulation Results Analysis. After the working face has advanced 30 m, the main roof had the first fracture. Broken rock masses on the main roof go down in a rotation manner. In this process, the main roof completely fall down along the coal wall and the cutting eye as a response to the hydraulic pressure (4.5 MPa) and dead load of the confined aquifer. Given that the loads on the broken rock masses of the key strata are relatively large, the broken rock masses cannot form the "Voussoir beam" and develop sliding instability (Figure 9).

To study the stress–displacement–fracture evolutionary characteristics of the overlying strata below the unconsolidated confined aquifer, two monitoring lines were set along the key strata, so the upper parts of the lower water-resisting layer can extract vertical stress and displacement. These lines can reflect the evolutionary characteristics of the overlying loads and subsidence of the key strata and the lower water-resisting layer. The evolutionary process of initiation, development, and connection of the fracture surface can be reflected by drawing the shear displacement on the joint. The model simulated evolutionary process of vertical stress of the overlying strata and fracture surface under different time steps is shown in Figure 10. The overlying loads above the gob and the lower water-resisting layer are listed in Table 3.

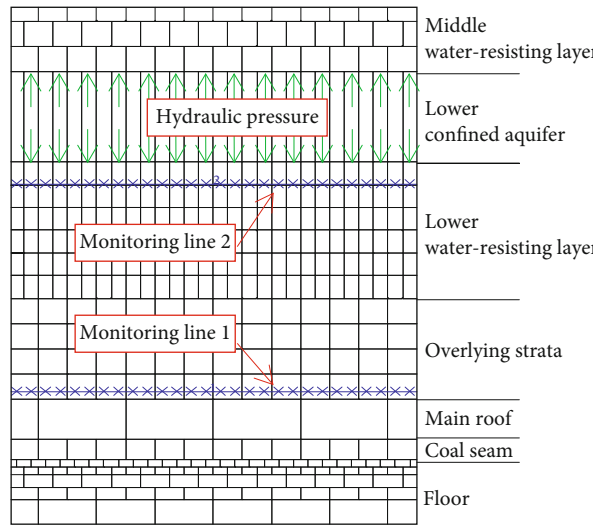

Figure 8: Numerical simulation model of mining below confined aquifer.

Figure 10 and Table 3 show that the original stress balance state surrounding the gob was damaged after the coal seam was recovered, which brought redistribution of stresses, thus causing deformation, failure, and movement of the overlying strata. After the working face advanced 30 m, the main roof developed the first breakage, and broken rock masses of the key strata slightly went down in rotation. This phenomenon can induce a significant unloading effect of the stope [25]. When the model was operated to the 250th time step, the overlying load of the key strata quickly decreases from 12.28 MPa before excavation to 1.36 MPa. Such unloading effect gradually weakens with the increase in roof height. The overlying load of the lower water-resisting layer decreased from 11.29 MPa before excavation to 7.54 MPa, and the rock strata moved to form mining fissures. Two vertical fracture surfaces were formed on the coal wall and above the cutting eye of the working face, with a

Table 1: Physical mechanical parameters of the block.

Lithology	h (m)	ρ (kg/m^{-3})	K (GPa)	G (GPa)	C (MPa)	ϕ (°)
Middle water-resisting layer	50	1800	2.70	1.30	0.50	15
Lower confined aquifer	18	2000	1.20	0.60	0.20	10
Lower water-resisting layer	27	1800	2.70	1.30	0.50	15
Overlying strata	20	2550	7.35	4.63	3.04	42
Main roof	8	2650	16.04	5.62	3.47	43
Coal seam	4	1400	1.90	0.93	0.80	27
Immediate floor	3	2500	3.94	2.60	1.68	30
Main floor	5	2600	7.94	6.31	2.93	35
Underlying strata	15	2600	10.92	3.72	2.10	43

h: thickness; ρ: density; K: bulk modulus; G: shear modulus; C: cohesion; and ϕ: friction angle.

Table 2: Mechanical parameters of the joint.

Lithology	Kn (GPa)	Ks (GPa)	C_j (MPa)	ϕ_j (°)
Middle water-resisting layer	3.5	1.8	0.12	8
Lower confined aquifer	2.0	1.2	0.08	5
Lower water-resisting layer	3.5	1.8	0.12	8
Overlying strata	4.0	2.0	0.20	8
Main roof	11.0	6.1	0.78	15
Coal seam	5.0	3.7	0.25	10
Immediate floor	7.5	4.4	0.46	12
Main floor	11.0	6.1	0.78	15
Underlying strata	14.0	8.7	0.65	18

Kn: normal stiffness; Ks: shear stiffness; C_j: cohesion of joint; and ϕ_j: friction angle of joint.

height reached as high as 34.5 m. The subsidence of the key strata further increased, while the overlying load of the key strata continued to decrease when the model operated to the 500th time step. However, the overlying load of the key strata decreased to 0.66 MPa under the gravity action of the overlying strata. The influencing height of strata unloading effect increased with the subsidence of the roof. The overlying load of lower water-resisting layer decreased to 4.58 MPa, and the development height of the fracture surface reached 37 m. As the model operated to the 1000th time step, the overlying load of key strata was kept at 0.78 MPa, but it was basically constant in the subsequent subsidence of overlying strata. The overlying load of the lower water-resisting layer continued to decrease because of the moving unloading effect of the strata, but it was kept at 4.40 MPa due to the hydraulic pressure. At the 2000th step, the development height of fracture surface reached 55 m, and it has run through the whole overlying strata. With the collaborative effect of dead load and hydraulic pressure, the slide mass overcame frictional forces of the rock masses on two sides of the fracture surface and generally moved downward. The overlying structure of the stope became instable. At the 8000th step, the falling gangues in the gob were compacted again, and the model had a balanced operation. The overlying loads of the key strata increased to 5.41 MPa.

The evolutionary process of shear displacement of the fracture surface at different operating time steps can be summarized by extracting the shear displacement on the joint. Figure 10 shows that before the 1000th time step, shear displacement on the bottom of joint continuously increased along the height direction during the balanced operation of the model, while the shear displacement on the top was approximately 0. Moreover, the slip dislocation on the joint developed upward, indicating that the fracture surface first occurred below the waterproof coal–rock pillar and continuously propagated upward. After the 1000th time step, shear displacement on the fracture surface was basically consistent in the upper and lower parts, except that the shear displacement synchronously increases with the balance operation of the model.

4. Water–Rock Coupling Induced Disaster Control Technique

The analysis indicated that the overlying strata structure stability below the confined aquifer is negatively related with the hydraulic pressure and breaking interval of the main roof, but it is positively related with the overlying strata strength and the waterproof coal–rock pillar height. Accordingly, the water bursting and powered support jammed accidents can be controlled by drainage for decreasing hydraulic pressure, presplitting blasting of the hard roof, grouting reinforced roof of the overlying strata, and increasing height of the waterproof pillar through redesigning. Moreover, numerical simulation on the control technique was carried out.

4.1. Drainage for Decreasing Hydraulic Pressure. Based on the initial model, the role of drainage for decreasing hydraulic pressure on the structure of the overlying structure in the stope was discussed by only changing the hydraulic pressure of the confined aquifer, while the other mining geological conditions were kept the same. Four models were reconstructed, in which the hydraulic pressures of the confined aquifer were 4.5 (simulated in the initial model), 2.5, 2.0, and 0.5 MPa. The distributions of vertical stress and fracture surfaces of the overlying rocks with different hydraulic are represented in Figure 11. The stress–displacement–fracture

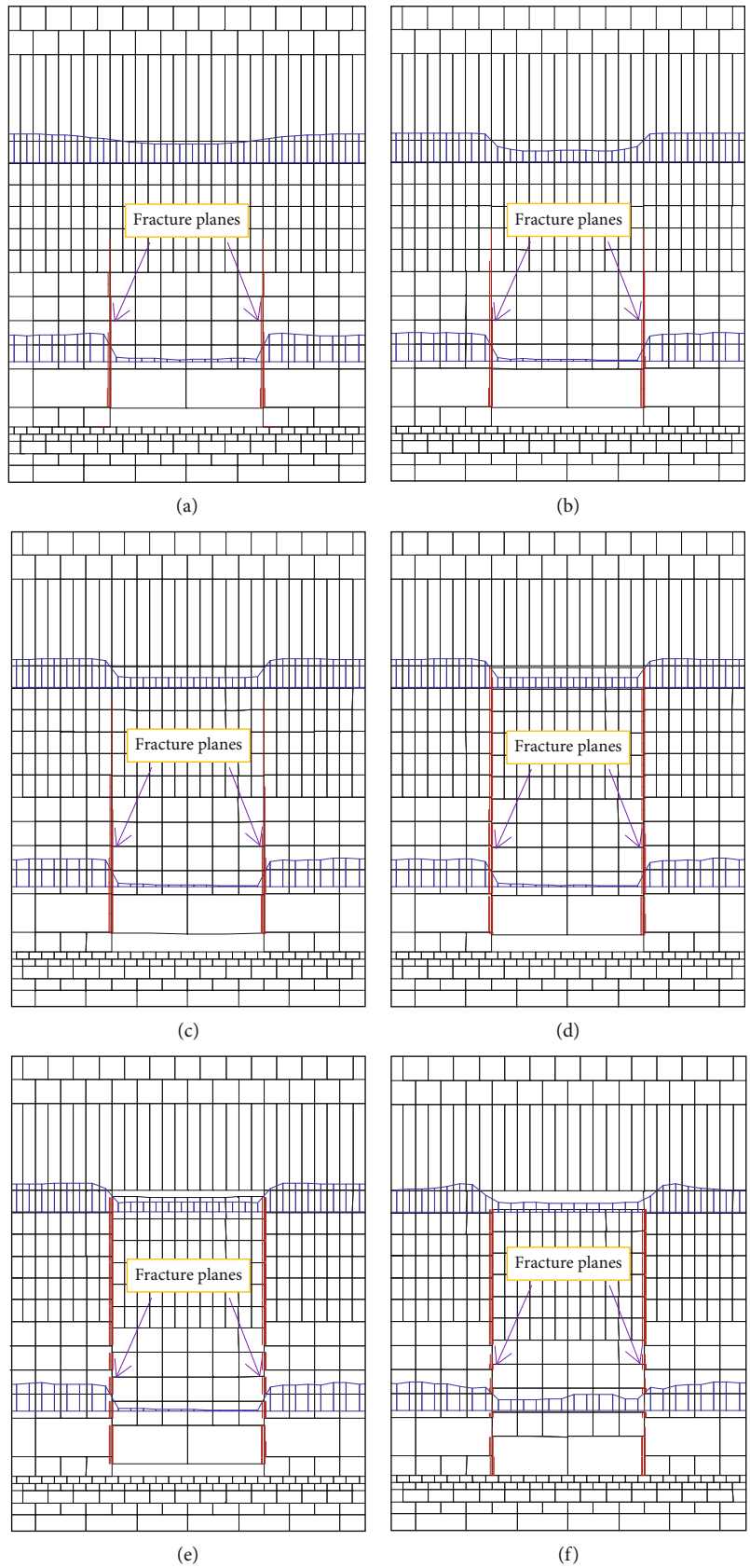

Figure 9: Evolution process of vertical stress and fracture planes of the overlying strata. (a) 250th step. (b) 500th step. (c) 1000th step. (d) 2000th step. (e) 4000th step. (f) 8000th step.

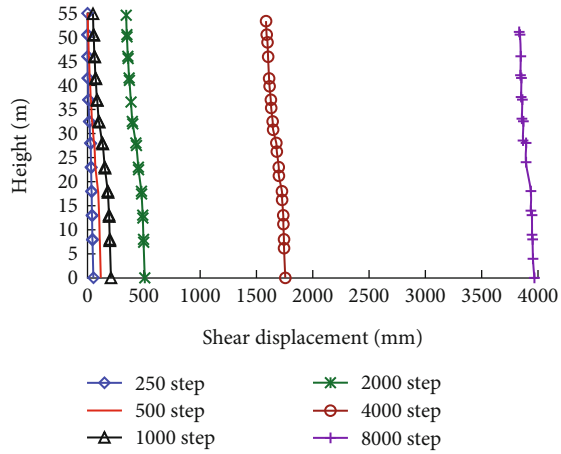

Figure 10: Evolution process of shear displacement on fracture planes.

Table 3: Pressure on the key strata and the lower water-resisting layer.

Time step (N)	Overlying load (MPa)	
	Key strata	Lower water-resisting layer
250	1.36	7.54
500	0.66	4.58
1000	0.78	4.40
2000	0.71	4.34
4000	0.79	4.34
8000	5.41	4.47
Premining	12.28	11.29

evolutionary characteristics under different hydraulic pressures are counted in Table 4.

Figure 11 and Table 4 demonstrate that the fracture surface runs through the whole waterproof coal–rock pillar under the water–rock coupling effect when the hydraulic pressure is higher than 2.5 MPa. The whole sliding body fell off and became instable due to the hydraulic pressure and dead load. Consequently, the working face developed the support jammed and water inrush accident. When the hydraulic pressure of the confined aquifer decreased to less than 2.0 MPa after drainage for decreasing hydraulic pressure, the overlying strata in the stope can form a balance structure. When the hydraulic pressure further decreases from 2.0 MPa to 0.5 MPa, the loads that were applied by the aquifer layer onto the lower water-resisting layer were still 2.2 MPa, higher than the hydraulic pressure. The fracture surfaces heights was 32.50 m, indicating that the hydraulic pressure of the aquifer layer did not play the role. The fracture surface failed to run through the whole waterproof coal–rock pillar, and the key strata only has to support the dead load and weights of the overlying strata.

4.2. Hard Roof Presplitting Blasting. The working face with a hard roof shortens the pressure step through presplitting blasting of the roof, thus enabling to relieve the strata pressure behaviors on the working face. During mining under the unconsolidated confined aquifer, the roof presplitting blasting can also improve the stability of the overlying strata structure. Four models were built, in which the first breaking intervals of the main roof were 30 (simulated in the initial model), 27, 25, and 20 m. The distributions of vertical stress of the overlying rocks in the stope and fracture surfaces under different first weighting intervals are shown in Figure 12. The stress–displacement–fracture evolutionary characteristics of the overlying strata under different first weighting intervals are counted in Table 5.

Figure 12 and Table 5 show that synchronous breakage of the overlying strata occurred at the first breakage of the main roof when the first weighting interval was larger than 27 m, accompanied by the overall falling instability of the waterproof coal–rock pillar. When the first breaking interval decreased to less 25 m after the deep-hole presplitting blasting of the hard roof, the overlying strata of the stope can form a balanced structure. When the breaking interval of the main roof is 25 m, the fracture development height was 51.63 m, and it nearly ran through the whole waterproof coal–rock pillar. The strata can balance the dead load and hydraulic pressure due to the frictional force of the rock masses at two sides of the sliding body. The sliding body was in the ultimate balancing state. The development height of the fracture surface was only 34.75 m when the breaking interval of the main roof was 20 m. The overlying strata in the stope was kept stable. The overlying loads of the key strata and the lower water-resisting layer were increased by 1.05 and 6.58 MPa, respectively. Although the overlying loads of the key strata increased, the it still could achieve a balance. This feature was mainly attributed to the decreased first breaking interval of the working face, the weakened unloading effect from mining, and the high overlying loads of the key strata and the lower water-resisting layer. Moreover, this feature proved that whether the breaking block of key stratum can form a balanced structure is related with not only the overlying loads but also its own stability.

4.3. Grouting Reinforced Roof of the Overlying Strata. Grouting reinforcement was performed to the weathering and oxidization belt by making grouting holes in the underground or ground. The strength reduction method was chosen in this study. First, the strength factor (k) was chosen to increase the strength parameters (c_j and φ_j) of the overlying rock according to Equation (3), followed by numerical calculation. In this way, the role of overlying strata strength on the stability of the overlying structure can be discussed. Four models were constructed, in which the k values were 1.0 (simulated in the initial model), 1.2, 1.5, and 2.0. The distributions of vertical stress of the overlying rocks in the stope and fracture surfaces under different overlying strata strengths are shown in Figure 13. The stress–displacement–-fracture evolutionary characteristics with different overlying strata strengths are counted in Table 6.

$$c_j' = kc_j \quad \phi_j' = \arctan\left(k \tan \phi_j\right). \tag{3}$$

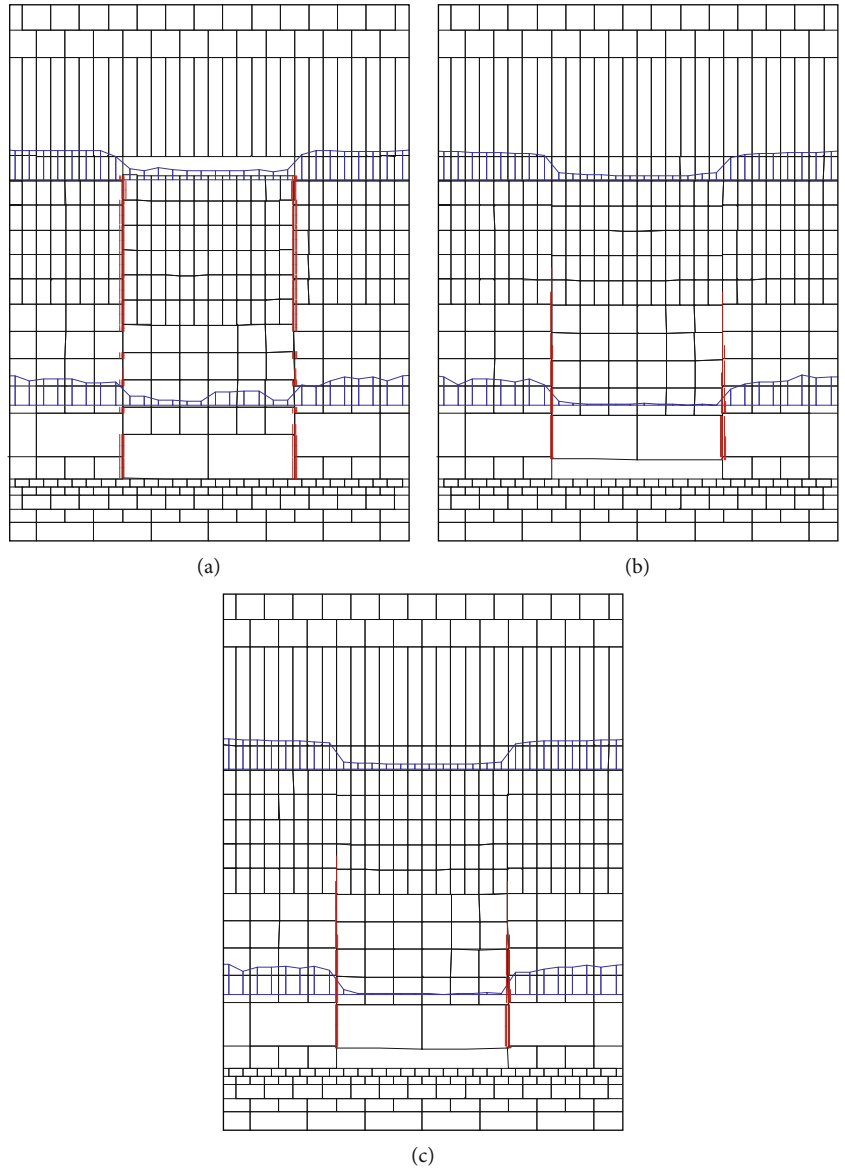

Figure 11: Distribution of vertical stress and fracture planes of the overlying strata with different hydraulic pressures. (a) 2.5 MPa. (b) 2.0 MPa. (c) 0.5 MPa.

Table 4: Influence of hydraulic pressure on the overlying strata structure stability.

Hydraulic pressure (MPa)	Overlying load (MPa)		Displacement (mm)		Fracture height (m)
	Key strata	Lower water-resisting	Key strata	Lower water-resisting	
4.5	5.41	4.47	3968.00	3877.00	55.00
2.5	3.43	2.51	3916.00	3702.00	55.00
2.0	0.47	2.16	393.00	115.90	32.50
0.5	0.58	2.20	371.30	83.94	32.50

Figure 13 and Table 6 show that the overlying strata in the stope formed a balanced structure when $k > 1.5$. When $k = 1.5$, the fracture development height was 53.88 m, and the fracture plane nearly ran through the whole waterproof coal–rock pillar. The sliding body was in the ultimate balance state. When $k = 2.0$, the development height of the fracture surface was only 39.25 m, and the overlying strata of the stope was kept stable. The shear strength among the broken rock masses increased with the increase in overlying strata strength, preventing further upward development of the

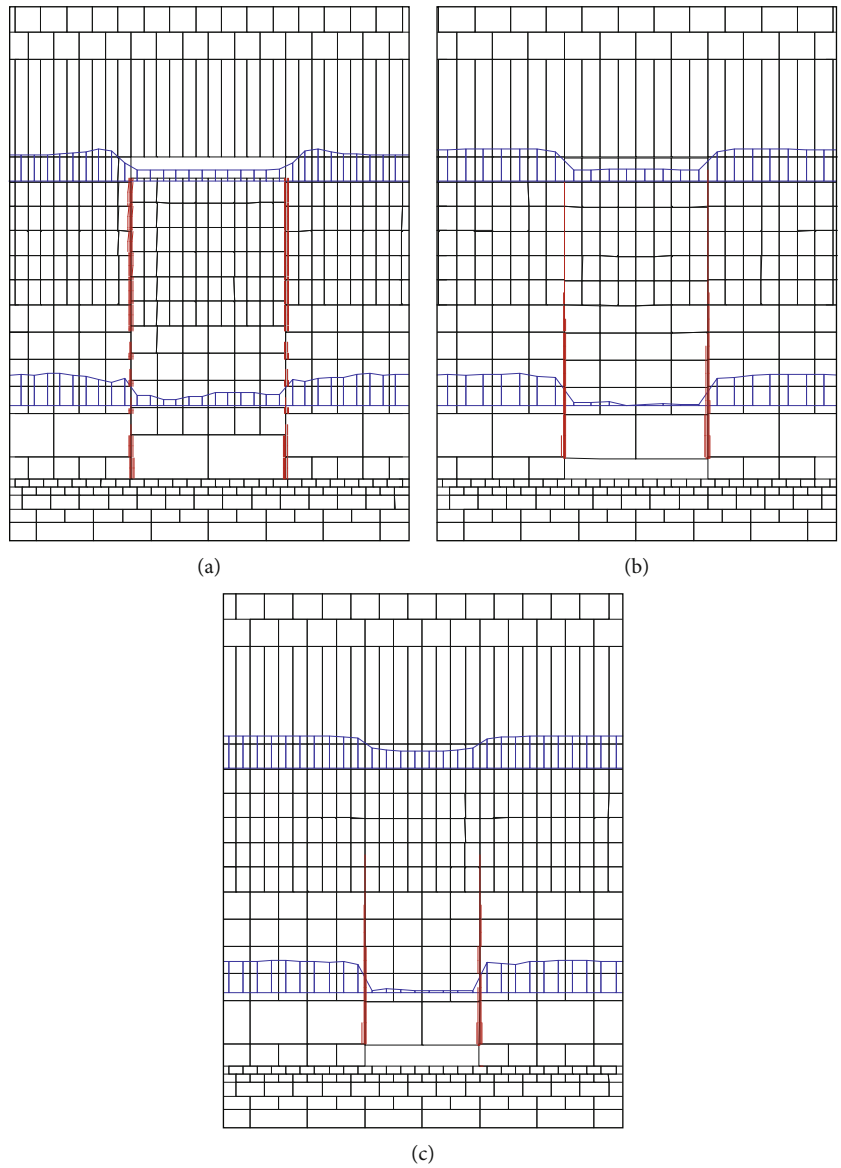

Figure 12: Distribution of vertical stress and fracture planes of the overlying strata with different first breaking intervals. (a) 27 m. (b) 25 m. (c) 20 m.

Table 5: Influence of the first breaking interval on the overlying strata structure stability.

Breaking interval (m)	Overlying load (MPa)		Displacement (mm)		Fracture height (m)
	Key strata	Lower water-resisting	Key strata	Lower water-resisting	
30	5.41	4.47	3968.00	3877.00	55.00
27	5.29	4.60	3955.00	3856.00	55.00
25	0.83	4.41	231.20	96.65	51.63
20	1.05	6.58	112.50	28.28	34.75

fracture surface. This condition was beneficial to maintain a balance of the overlying structure in the stope.

4.4. Increasing Height of the Waterproof Coal–Rock Pillar. Four models were constructed, in which the heights of the waterproof coal–rock pillars were 55 (simulated in the initial model), 70, 85, and 100 m. The distributions of vertical stress of the overlying rocks in the stope and fracture surfaces under different heights of waterproof coal–rock pillars are shown in Figure 14. The stress–displacement–fracture evolutionary with different waterproof coal–rock pillars heights is counted in Table 7.

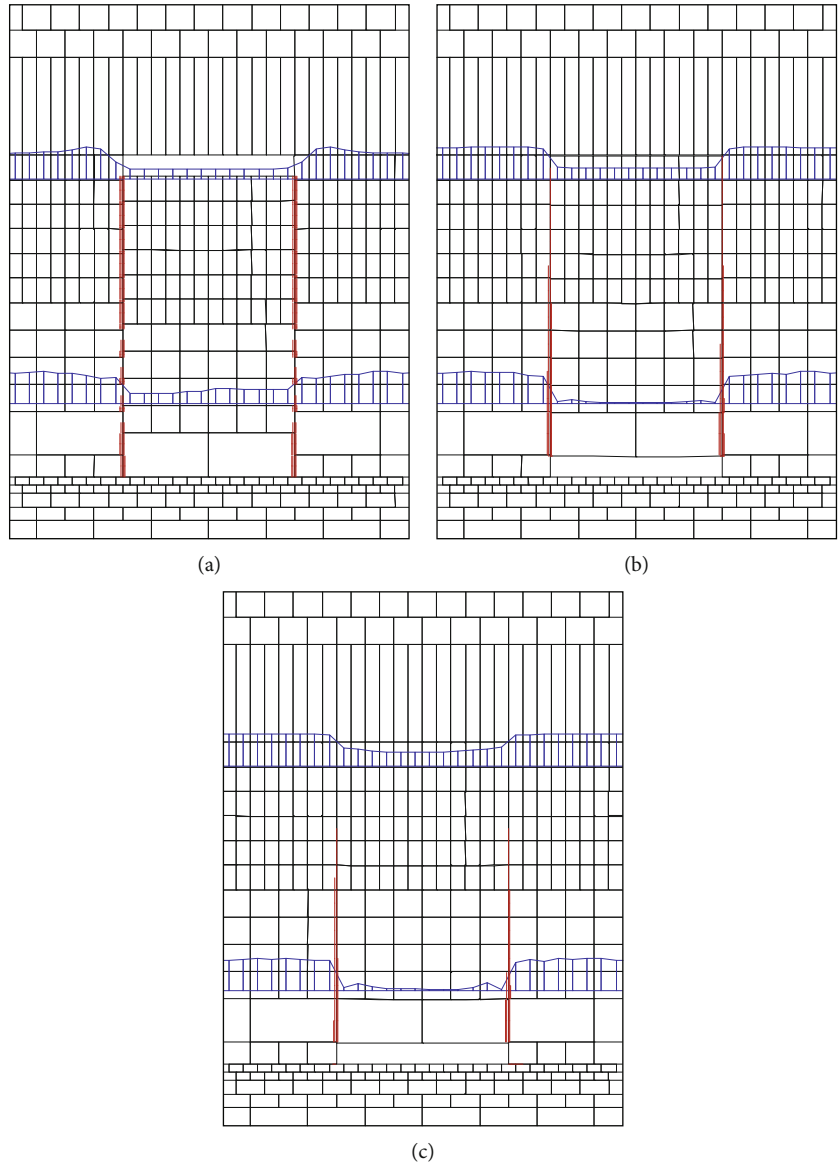

Figure 13: Distribution of vertical stress and fracture planes of the overlying strata with different strength enhancement factors. (a) 1.2. (b) 1.5. (c) 2.0.

Table 6: Influence of the strength enhancement factor on the overlying strata structure stability.

Strength enhancement factor	Overlying load (MPa)		Displacement (mm)		Fracture height (m)
	Key strata	Lower water-resisting	Key strata	Lower water-resisting	
1.0	5.41	4.47	3968.00	3877.00	55.00
1.2	5.42	4.40	3963.00	3879.00	55.00
1.5	0.87	4.42	207.70	112.20	53.88
2.0	0.71	5.89	120.10	42.75	39.25

Figure 14 and Table 7 show that the overlying strata was still cut down and became instable when the waterproof coal–rock pillars increased from 55 m to 70 m. The fracture development height was 70 m, which ran through the whole overlying strata. When the waterproof coal–rock pillar was 85 m, the fracture surface was only 64.75 m, and a 20.25 m thick strata can be found above the water-resisting layer, which did not crack and develop deformation failures. The overlying strata in the stope were kept stable. When the waterproof coal–rock pillar increased to 100 m, the fracture surface also increased to 74.13 m. However, it only ran through the overlying strata, and the lower water-resisting

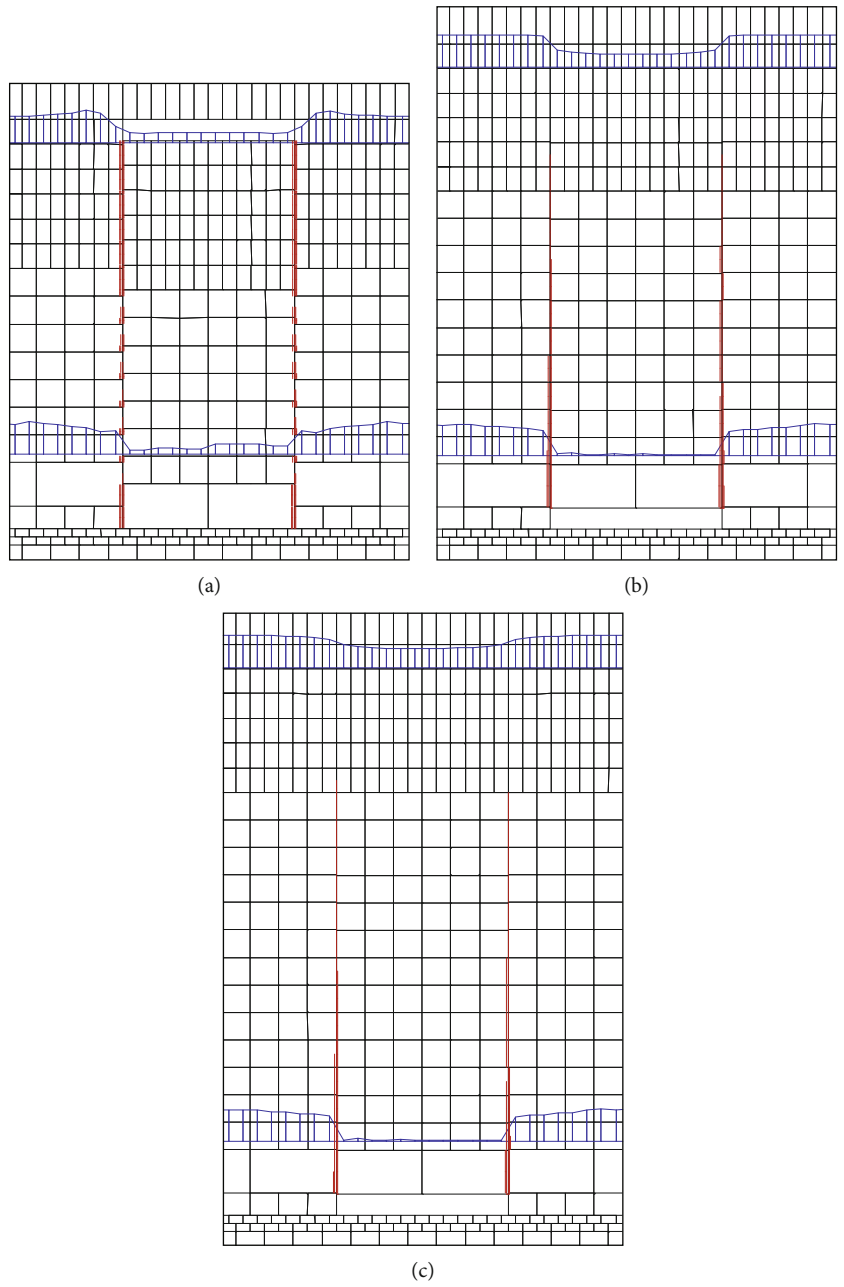

Figure 14: Distribution of vertical stress and fracture planes of the overlying strata with different heights of the waterproof coal pillars. (a) 70 m. (b) 85 m. (c) 100 m.

Table 7: Influence of the height of the waterproof coal pillar on the overlying strata structure stability.

Height of waterproof coal pillar (m)	Overlying load (MPa)		Displacement (mm)		Fracture height (m)
	Key strata	Lower water-resisting	Key strata	Lower water-resisting	
55	5.41	4.47	3968.00	3877.00	55.00
70	3.49	4.59	3956.00	3839.00	70.00
85	0.60	5.26	177.60	45.72	64.75
100	0.59	6.83	151.90	33.48	74.13

layer was kept integral. The overlying load of the key strata was 0.59 MPa, and the breaking block of the key stratum could form a stable "Voussoir beam" structure.

5. Field Applications

5.1. Case 1. The width was 195 m of 1512(3) working face in Huainan Gubei Mine, and the recoverable length was 392 m [12]. The coal seam thickness was 4.5 m, and the dip angle was 5° in average. The waterproof coal pillar at the upper end of the cutting eye was 50 m, and the range from 20 m to 50 m above the roof was the weathering and oxidization belt.

Only 20 m of hard rocks can be found above the coal seam on working face 1512(3). At the first breakage of the main roof, the weathering and oxidization belt in the overlying strata cannot easily form a "pressure arch" bearing structure, and it may develop the sliding instability. To improve strength of the weathering and oxidization belt, Gubei Mine applied the directional drilling technology and horizontal pregrouting technology. Ground pregrouting reinforcement was used to the weathering and oxidization belt [12], which increased the shear strength of the weathering mudstone and assured smooth recovery of working face 1512(3).

5.2. Case 2. The 1312(1) working face in Gubei Mine was the first mining face in the Nanyi (11-2) mining area. The coal seam was 1.8–4.0 m thick, averaging at 3.6 m. The dip angle was 3°–7°, 5° in average. The elevation of the bedrock surface at the upper end of the cutting eye was −426.8 m, and that of the roof of the 11-2# coal seam was −454.9 m. The minimum height of the waterproof coal pillar was 28.1 m.

According to the histogram of the 2# drill at the cutting eye on 1312(1) working face, 6.0 m thick siltstone, 2.0 m sandy mudstone, 4.0 m fine sandstone, 2.0 m sandy mudstone, 3.0 m mudstone, and 2.0 m fine sandstone can be found from the bottom to the upper confined aquifer. Based on the analysis, the 6.0 m thick siltstone is the main roof. The thick and hard main roof led to the great first weighting interval and obvious strata pressure behaviors on the working face. To shorten the first weighting interval and decrease the pressure strength of the working face, deep-hole presplitting blasting was performed at the cutting eye for forced caving. The diameter and depth of the explosive hole were 75 mm and 20 m. Moreover, the hole sealing length, loading length, explosive load/hole, angle of elevation (relative to the horizontal plane), and weakening height of the roof were set to 6 m, 14 m, 42 kg, 49°, and 15 m, respectively. The space between the explosive holes was 15 m, and a total of 12 explosive holes were set along the cutting eye.

The mining practices have proven that after the deep-hole presplitting blasting, the first weighting interval was decreased by 23 m, and the strata pressure behaviors were not obvious in the pressure period. This result indicated that the presplitting blasting parameters were reasonably designed, and it did not cause overall movement of the overlying strata during the first breakage of the main roof. The presplitting blasting of the roof has achieved good results.

6. Conclusions

(1) The overlying strata structural instability below the unconsolidated confined aquifer is related with the unique roof strata conditions and hydrogeological conditions of working faces

(2) The stability of the overlying strata structure by the water–rock coupling effect reduces with increasing hydraulic pressure and breaking interval of the main roof and decreasing overlying strata strength and height

(3) After the first breakage of the main roof, two vertical fracture surfaces are formed above the coal wall and the cutting eye of the working face. These two surfaces gradually propagate upward. The overlying strata structure of the stope remains stable before the fracture surfaces run through the whole waterproof coal–rock pillar

(4) After the fracture surfaces run through the whole waterproof coal–rock pillar, the overlying strata structure of the stope still remains stable if the hydraulic pressure of the confined aquifer is small. The sliding body is in the ultimate balance state when its dead load and overlying loads achieve a balance with the frictional forces of the rock masses at two sides

(5) The working face develops power support jammed and water inrush accidents when the hydraulic pressure of the confined aquifer is relatively high. The sliding body falls and becomes instable due to the hydraulic pressure of the confined aquifer and dead loads of the sliding body

(6) Power support jammed and water inrush accidents can be prevented by drainage for decreasing hydraulic pressure, presplitting blasting of the hard roof, grouting reinforced roof of the overlying strata, and increasing the waterproof coal–rock pillar height

Data Availability

The data used to support the findings of this study are available from the corresponding author upon request.

Conflicts of Interest

The authors declare that there are no conflicts of interest regarding the publication of this paper.

Acknowledgments

This work was supported by the State Key Research Development Program of China (2019YFC1904304), National Natural Science Foundation for Young Scientists of China (51604008), and Institute of Energy, Hefei Comprehensive National Science Center (19KZS203), all of whom are gratefully acknowledged.

References

[1] State Administration of Work Safety, *State Administration of Coal Mine Safety*, Rule of Mine Prevention and Cure Water Disaster, China Coal Industry Publishing House, Beijing, China, 2009.

[2] L. Yuan and M. C. Liu, "Discussion on reducing waterproof pillaring on part block in Panji mining area," *Coal Science and Technology*, vol. 27, no. 1, pp. 32–35, 1999.

[3] W. Y. Zhang, W. G. Wang, W. D. Peng, Z. H. Feng, and K. S. Shu, "The coal mining practice of reducing waterproof coal pillars in Panxie mining area," *Journal of China Coal Society*, vol. 27, no. 2, pp. 128–133, 2002.

[4] P. Q. Li, "Coal mining under surface water bodies in Huainan mining area practice and inspiration," *Journal of Chine Coal*, vol. 27, no. 4, pp. 30–32, 2001.

[5] J. B. Li, K. Yang, J. L. Hou, and J. Li, "Verification and analysis on upper limit increased coal mining method in coal mining face of Panbei mine," *Coal Science and Technology*, vol. 40, no. 2, pp. 25–28, 2012.

[6] X. Y. Xiong and J. B. Li, "A case study of support break-off at 1402(3) fully mechanized mining face," *Coal Geology of China*, vol. 16, no. 3, pp. 34–37, 2004.

[7] Z. H. Li, X. Z. Hua, K. Yang, and S. W. Ge, "Risk evaluation of powered support jammed in working face with a raise of mining upper limit based on comprehensive index method," *Journal of Mining and Safety Engineering*, vol. 32, no. 3, pp. 389–395, 2015.

[8] B. S. Yang, X. Y. Liu, C. G. Yin, C. Y. Yan, and G. L. Liang, "Characteristics of strata behaviors and surrounding rock control in upper exploitation limitation-heightened working face," *Ground Pressure and Strata Control*, vol. 2, pp. 58-59, 2000.

[9] J. L. Xu, W. B. Zhu, and X. Z. Wang, "Study on water-inrush mechanism and prevention during coal mining under unconsolidated confined aquifer," *Journal of Mining and Safety Engineering*, vol. 28, no. 3, pp. 333–339, 2011.

[10] J. L. Xu, J. X. Chen, and K. Jiang, "Effect of load transfer of unconsolidated confined aquifer on compound breakage of key strata," *Chinese Journal of Rock Mechanics and Engineering*, vol. 26, no. 4, pp. 699–704, 2007.

[11] J. L. Hou, G. X. Xie, Y. Z. Tang et al., "Three-dimensional mechanical characteristics of rocks surrounding the stope of thick unconsolidated layers and thin bedrock," *Journal of China Coal Society*, vol. 38, no. 12, pp. 2113–2118, 2013.

[12] H. L. Zhang, M. Tu, H. Cheng, and Y. Z. Tang, "Breaking mechanism of overlying strata under thick unconsolidated layers and integrated grouting reinforvcement technology for wind oxidation zong," *Journal of China Coal Society*, vol. 43, no. 8, pp. 2126–2132, 2018.

[13] F. F. Meng, H. Pu, J. R. Chen, and C. Xiao, "Extension law of thin bedrock fissure based on particle discrete element," *Journal of China Coal Society*, vol. 42, no. 2, pp. 421–428, 2017.

[14] D. S. Zhang, W. P. Li, X. P. Lai, G. W. Fan, and W. Q. Liu, "Development on basic theory of water protection during coal mining in northwest of China," *Journal of China Coal Society*, vol. 42, no. 1, pp. 36–43, 2017.

[15] J. Zhang, T. Yang, Y. L. Suo, D. Liu, and F. W. Zhou, "Roof water-inrush disaster forecast based on the model of aquiclude instability," *Journal of China Coal Society*, vol. 42, no. 10, pp. 2718–2724, 2017.

[16] Y. C. Xu, M. Z. Du, J. H. Li, and X. C. Cao, "Instability mechanism and design method of coal and rock pillar under hydraulic pressure," *Journal of China Coal Society*, vol. 42, no. 2, pp. 328–334, 2017.

[17] X. Z. Wang, J. L. Xu, Y. H. Wu, H. Wang, H. K. Han, and Y. M. Ji, "The influence of repeated mining on failure characteristic of overburden strata under unconsolidated confined aquifer," *Journal of Mining and Safety Engineering*, vol. 34, no. 3, pp. 437–443, 2017.

[18] X. Z. Wang, J. L. Xu, W. B. Zhu, and Y. C. Li, "Roof preblasting to prevent support crushing and water inrush accidents," *International Journal of Mining Science and Technology*, vol. 22, no. 3, pp. 379–384, 2012.

[19] Q. X. Huang, "Ground pressure behavior and definition of shallow seams," *Chinese Journal of Rock Mechanics and Engineering*, vol. 21, no. 8, pp. 1174–1177, 2002.

[20] Z. J. Hou, "Study on key strata in shallow seam," *Journal of China Coal Society*, vol. 24, no. 4, pp. 359–363, 1999.

[21] M. G. Qian and P. W. Shi, *Underground Pressure and Strata Control*, China University of Mining and Technology Press, Xuzhou, China, 2003.

[22] Z. H. Li, X. Z. Hua, K. Yang, and B. Qian, "Relation between support and surrounding rocks and its influence on strata behaviors in working face with a raise of mining upper limit," *Chinese Journal of Rock Mechanics and Engineering*, vol. 34, no. 6, pp. 1162–1171, 2015.

[23] M. R. Shen, *Rock Mass Mechanics*, Tongji University Press, Shanghai, China, 1999.

[24] K. Yi, P. L. Gong, and C. Liu, "Overlying strata structures and roof control of working face under thin topsoil and thin bedrock in shallow seam," *Journal of China Coal Society*, vol. 43, no. 5, pp. 1230–1237, 2018.

[25] F. S. Li, Y. Zhang, and L. F. Xu, "Influence of ratio of basement and loadings on mining face rock pressure in thin basement rock thick surface soil," *Journal of China Coal Society*, vol. 38, no. 10, pp. 1749–1755, 2013.